Infrared absorption from OH^- ions adjacent to lithium acceptors in hydrothermally grown ZnO

L. E. Halliburton,[a] Lijun Wang, Lihua Bai, N. Y. Garces, and N. C. Giles
Department of Physics, West Virginia University, Morgantown, West Virginia 26506

M. J. Callahan
Air Force Research Laboratory, Sensors Directorate, Hanscom Air Force Base, Massachusetts 01731

Buguo Wang
Solid State Scientific, Nashua, New Hampshire 03049

(Received 17 May 2004; accepted 20 August 2004)

An intense infrared absorption band has been observed in a hydrothermally grown ZnO crystal. At 12 K, the band peaks near 3577.3 cm^{-1} and has a half width of 0.40 cm^{-1}, and at 300 K, the band peaks at 3547 cm^{-1} and has a half width of 41.3 cm^{-1}. This absorption band is highly polarized, with its maximum intensity occurring when the electric field of the measuring light is parallel to the *c* axis of the crystal. Photoinduced electron-paramagnetic-resonance experiments show that the crystal contains lithium acceptors (i.e., lithium ions occupying zinc sites). Lithium and OH^- ions are present in the crystal because lithium carbonate, sodium hydroxide, and potassium hydroxide are used as solvents during the hydrothermal growth. In the as-grown crystal, some of the lithium acceptors will have an OH^- ion located at an adjacent axial oxygen site (to serve as a passivator), and we assign the 3577.3-cm^{-1} band observed at 12 K to these neutral complexes. Our results illustrate the role of hydrogen as a charge compensator for singly ionized acceptors in ZnO. © *2004 American Institute of Physics*. [DOI: 10.1063/1.1806531]

I. INTRODUCTION

The role of hydrogen in zinc oxide continues to be a subject of considerable interest. Recent first-principles calculations by Van de Walle[1–4] strongly suggested that hydrogen acts as a donor in ZnO. This theoretical work has prompted a series of experimental investigations[5–22] of the behavior of hydrogen in ZnO using techniques such as electron paramagnetic resonance (EPR), electron-nuclear double resonance, infrared absorption spectroscopy, Raman backscattering spectroscopy, photoluminescence, temperature-dependent Hall, deep-level transient spectroscopy, cathodoluminescence, secondary-ion mass spectrometry, and Rutherford backscattering/channeling. In some of these studies, ion implantation and exposure to hydrogen plasmas were used to incorporate hydrogen into bulk crystals. Hydrogen in ZnO was also a focus of earlier studies. In the 1970s, EPR, infrared absorption, and conductivity experiments were conducted on crystals simultaneously doped with copper and hydrogen.[23–26] However, despite the significant attention being given to hydrogen, especially in the last several years, the details of how this important impurity directly affects the various electrical and optical properties of ZnO crystals are not well established.

In the present paper, we describe the results of an infrared absorption and EPR study of a hydrothermally grown ZnO crystal. This growth technique is able to produce large, high-quality single crystals.[27] We have characterized an intense OH^- absorption line, present in the as-grown material, that peaks near 3577.3 cm^{-1} at 12 K. This band was previously observed by Lavrov[11] in a hydrothermally grown ZnO crystal and he suggested that it may represent a Ni–H complex. Our results indicate that an alternative model is needed because there is very little nickel present in our crystals. At 300 K, the infrared band we have studied shifts to 3547 cm^{-1} and broadens. We believe that the absorption band described in our present paper is the same as the room-temperature band previously reported by Seager and Myers[12] at 3546 cm^{-1} in hydrothermally grown crystals. These latter investigators postulated that their infrared band was due to a hydrogen located in a bond-centered position between oxygen and zinc atoms (thus representing hydrogen as a donor) while allowing that the band might contain unresolved components from some OH^- ions having an acceptor replacing the zinc. Because this particular infrared absorption band has not been observed in ZnO crystals grown by techniques other than hydrothermal, we propose a model that directly involves a specific acceptor impurity. EPR results show that neutral lithium acceptors can be photoinduced in our ZnO crystal (thus verifying that the hydrothermal growth process introduces significant amounts of lithium), and we assign the 3577.3-cm^{-1} infrared absorption band to a neutral complex consisting of a singly ionized lithium acceptor and an OH^- ion on an adjacent oxygen site. An analogous $Li–OH^-$ defect has been observed in MgO crystals.[28,29] An estimate of the concentration of OH^- ions contributing to our 3577.3-cm^{-1} band is made.

II. EXPERIMENTAL DETAILS

The bulk ZnO sample used in the present study was cut from the $+c$ region of a boule grown by the hydrothermal

[a]Electronic mail: larry.halliburton@mail.wvu.edu

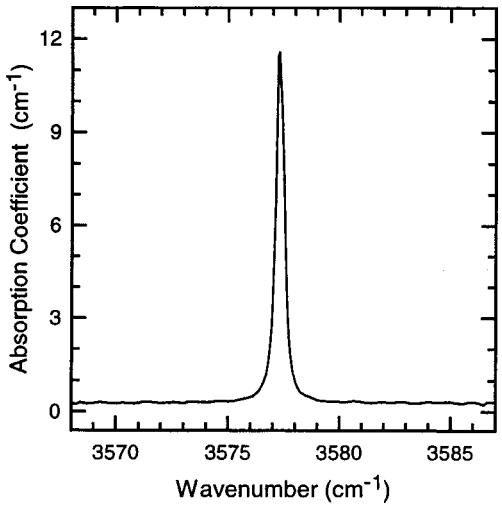

FIG. 1. Infrared absorption spectrum from a hydrothermally grown ZnO crystal, taken at 12 K using a polarizer. The electric field of the measuring light was oriented parallel to the c axis ($E \| c$). The peak of the OH^- band occurs at 3577.3 cm^{-1}. This band cannot be observed when the polarizer is rotated to $E \perp c$.

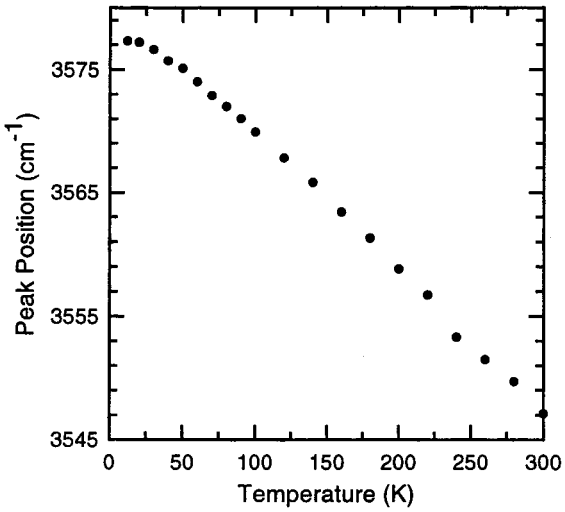

FIG. 2. Temperature dependence of the peak position of the dominant OH^- band in a hydrothermally grown ZnO crystal.

method[30] at the Air Force Research Laboratory (Hanscom AFB, MA). A welded platinum cylinder with an inside diameter of approximately 4.4 cm and a volume of 500 cm^3 was held in a larger autoclave. The seed crystal was a (0001) plate, the initial fluid fill was 80%, and the solvent (i.e., mineralizer) was 3M NaOH, 1M KOH, and 0.5M Li_2CO_3. The temperatures in the nutrient and in the growth zones were 355 and 345 °C, respectively, and the growth rate along the $+c$ axis was approximately 0.2 mm/day.

A small sample, with approximate dimensions of $4.5 \times 3.4 \times 2.9$ mm^3, was used in the infrared absorption and EPR experiments. The absorption data were taken with a ThermoNicolet Nexus 870 Fourier-transform infrared spectrometer (using a KBr beamsplitter and a cooled HgCdTe detector). A ZnSe wire-grid polarizer from Molectron (Model IGP-229) was placed in the incident beam path. The EPR data were obtained using a Bruker EMX spectrometer operating near 9.45 GHz. Oxford Instruments helium-gas flow systems were used to control the sample temperature in both the absorption and EPR experiments. A cw helium-cadmium laser (operating at 442 nm) was used to produce the paramagnetic (i.e., neutral) charge state of the lithium acceptors for the EPR studies.

III. RESULTS

Figure 1 shows the intense infrared absorption band occurring at 3577.3 cm^{-1} in our hydrothermally grown ZnO crystal. These data were taken at 12 K with the electric field of the polarized incident light oriented parallel to the c axis of the crystal. The sample thickness (i.e., the optical path length) was 4.5 mm. The width of the line (measured at the half-maximum points) is 0.40 cm^{-1}, which we note is near the 0.125-cm^{-1} instrument resolution of our spectrometer. In addition to a very large intensity, the most unique feature of the infrared absorption band at 3577.3 cm^{-1} is its high degree of polarization. We were unable to observe this band in our samples when the polarizer was rotated 90° (thus making the electric field of the polarized incident light perpendicular to the c axis). Nor could it be observed in separate experiments where the polarizer was removed from the spectrometer and the measuring light propagated along the c axis of the crystal. Other infrared absorption bands observed in our sample (but not shown) were a weak signal near 6005 cm^{-1} that has been assigned to Co^{2+} ions[31] and a weak signal near 4240 cm^{-1} that has been assigned to Ni^{2+} ions.[11,32] The Ni^{2+} signal was approximately 440 times smaller than the 3577.3-cm^{-1} band.

As the temperature increased, the peak position of our dominant infrared absorption band shifted to lower frequency. This effect is shown in Fig. 2, where the peak position is plotted as a function of the temperature. The peak position shifts from 3577.3 cm^{-1} at 12 K to 3547 cm^{-1} at 300 K. A significant broadening of the band also occurs as the temperature is increased. These results are shown in Fig. 3, where the width broadens from 0.40 cm^{-1} at 12 K to

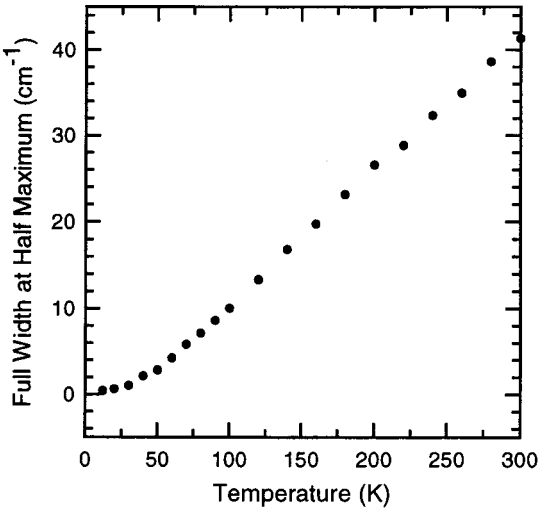

FIG. 3. Temperature dependence of the width of the OH^- band (measured at the half-maximum points).

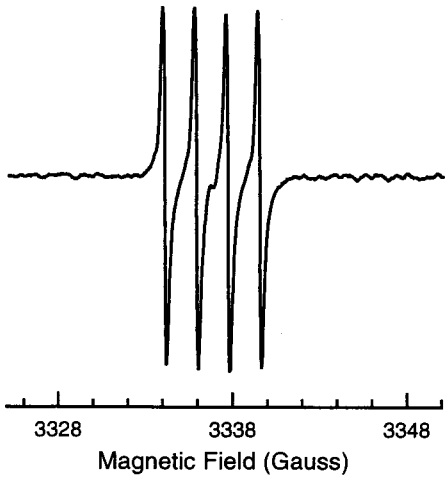

FIG. 4. EPR spectrum of the axial neutral lithium acceptor. These data were taken at 40 K during exposure to 442-nm laser light. The magnetic field was perpendicular to the *c* axis.

41.3 cm^{-1} at 300 K. The data in Figs. 2 and 3 were taken with the polarizer oriented such that the electric field of the incident light was parallel to the *c* axis. Because of the broadening, this infrared absorption band is not expected to be easily seen at room temperature in ZnO crystals.

A series of EPR experiments provided additional information about the point defects present in our hydrothermally grown ZnO crystal. Relatively strong EPR spectra from Fe^{3+}, Mn^{2+}, and Co^{2+} ions were observed near 40 K in the as-grown crystal.[33–35] The combined concentrations of these impurities was estimated from EPR to be approximately 1–2 ppm. A weak EPR signal from Ni^{3+} ions[36] was also observed at low temperature (representing a concentration less than 0.02 ppm). A signal at $g=1.96$ due to shallow donors[37,38] was small, but easily seen, in our crystal, thus indicating that it was electrically *n* type. A value of 2×10^{15} cm^{-3} was obtained for the room-temperature Hall electron carrier concentration.

Photoinduced EPR experiments were also performed on our hydrothermally grown crystal. When the crystal was exposed to 442-nm light at 40 K, an EPR signal due to the neutral lithium acceptors appeared. This "light-on" spectrum, taken at 40 K with the magnetic field oriented perpendicular to the *c* axis, is shown in Fig. 4. The four-line hyperfine pattern is due to the interaction between the unpaired spin and the ^{7}Li nucleus ($I=3/2$, 92.5% abundant). We estimate that the concentration of the photoinduced neutral lithium acceptors in our crystal was approximately 1.3×10^{15} cm^{-3}. An increase in the shallow donor EPR signal and a decrease in the Fe^{3+} EPR signal were observed to coincide with the production of the neutral lithium acceptors, thus indicating that electrons were being temporarily trapped in the form of neutral shallow donors and as Fe^{2+} ions. It is important to note that even though the neutral lithium acceptor may be present at lower temperatures during and after optical excitation, its EPR spectrum cannot be easily observed at temperatures below 30–40 K because of the severe microwave saturation effects resulting from the extremely long spin-lattice relaxation times at the lower temperatures.

As reported by Schirmer,[39] the neutral lithium acceptor has the hole localized on only one of its four adjacent oxygen ions instead of being shared nearly equally by these four neighboring anions. This gives rise to two distinct (i.e., very similar but slightly different) neutral lithium acceptors. When the hole resides on one of the three neighboring oxygen ions located in the basal plane, the resulting neutral acceptor is referred to as a "nonaxial" lithium center. These nonaxial centers form a set of three crystallographically equivalent but magnetically inequivalent centers because of the three possible sites for the hole relative to the lithium. The fourth oxygen ion neighboring the lithium has a slightly different bond length from the other three oxygens. When the hole resides on this oxygen (located along the *c* axis relative to the lithium ion), the resulting neutral acceptor is referred to as an "axial" lithium center. Schirmer[39] has shown that the ground-state energies of the axial and nonaxial lithium centers differ by 15 meV, with the axial form being the lowest in energy. The EPR spectrum shown in Fig. 4 represents the axial neutral lithium acceptors. Earlier donor-acceptor-pair recombination and thermoluminescence experiments that monitored the lithium-associated yellow emission provided evidence that the large lattice relaxation accompanying the localization of the hole on a single oxygen neighbor makes lithium a deep acceptor in ZnO.[40–42] The ionization energy of the lithium acceptor in ZnO is estimated to be between 600 and 800 meV.

IV. DISCUSSION

The low-temperature infrared absorption band we have observed at 3577.3 cm^{-1} represents the fundamental stretching vibration of an OH^- ion. Direct evidence for this assignment has been provided by Lavrov.[11] He produced the low-temperature OD^- version of this band at 2644.4 cm^{-1} during a deuterium-plasma treatment of a hydrothermally grown crystal. We also note that the peak position of 3577.3 cm^{-1} is very near the experimental value of 3555.6 cm^{-1} obtained for a free OH^- ion using high-precision gas phase spectroscopy.[43] In general, it is very common to observe OH^- ions in oxide crystals, and a recent review of this subject has been provided by Wohlecke and Kovacs.[44] They discuss the isotope, anharmonic, temperature, and polarization effects found in these vibrating systems, and they describe specific models associated with OH^- ions in various oxide compounds. A comprehensive review of hydrogen in nonoxide crystalline semiconductors has been provided by Pearton *et al.*[45]

The infrared absorption band we describe in the present paper has been previously observed by Lavrov[11] at 10 K and by Seager and Myers[12] at room temperature. In both of those cases, as well as our own, the crystals were grown by the hydrothermal technique. Thus far, this band has not been observed in crystals grown by other techniques. Lavrov[11] suggested that the band was due to a $Ni-OH^-$ complex, but we find very little nickel in our samples (i.e., we could barely detect the Ni^{2+} absorption near 4240 cm^{-1}). Seager and Myers[12] proposed that the band was due to a hydrogen located in a bond-centered position between oxygen and zinc

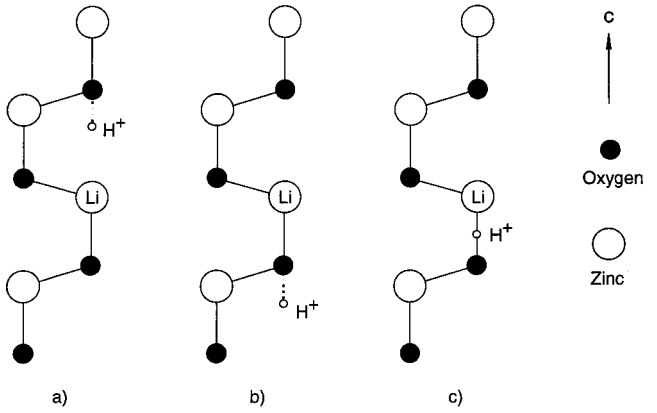

FIG. 5. Possible models for the lithium-associated OH^- ion in hydrothermally grown ZnO. In each case, the lithium ion occupies a zinc site. (a) The OH^- ion is on the nearest axial nonbonding oxygen site with the proton facing the lithium. (b) The OH^- ion is on the nearest axial bonding oxygen site with the proton extending out opposite the lithium. (c) The proton occupies a bond-center position immediately adjacent to the lithium. An expected lattice distortion of the lithium is not shown in this last model.

atoms (similar to the $BC_{\|}$ configuration in the calculations of Van de Walle[1]). However, this describes a general defect that would be expected to be present in all ZnO crystals containing hydrogen instead of only those grown hydrothermally. Seager and Myers[12] also suggested that the observed band could be due to a slightly different model in which the zinc is replaced by an acceptor. We agree with this focus on acceptors and offer a model that is specific to hydrothermally grown crystals and, by extension, to crystals that may have been doped with lithium and hydrogen during the growth itself or during postgrowth-diffusion treatments.

Lithium ions are present in large concentrations in nearly all hydrothermally grown ZnO crystals because of the use of lithium-containing compounds as solvents during growth. A portion of these ions are isolated singly ionized lithium acceptors (in ionic terms, this is a Li^+ ion replacing a Zn^{2+} ion with no local charge compensation and, in semiconductor terms, this is an A^- center). The photoinduced EPR data in Fig. 4 verifies that these isolated lithium ions are initially present in our crystal and that they can be converted to neutral lithium acceptors at low temperature by trapping a hole. Other lithium ions in the as-grown crystal will have an adjacent OH^- ion and, thus, will not form the paramagnetic neutral acceptors under illumination. These protons enter the lattice during the hydrothermal growth (either as OH^- ions, hydrogen atoms, or H_2O molecules) and are attracted to the singly ionized lithium acceptors. In ionic terms, the Li^+ ion has an effective negative charge relative to the lattice (i.e., it replaces a Zn^{2+} ion) and it electrostatically attracts the positively charged proton. The complex formed by the singly ionized lithium acceptor and the OH^- ion on an adjacent oxygen site is neutral, and, thus, is not expected to show electrical activity. We assign the 3577.3-cm^{-1} infrared absorption band to the OH^- ion that participates in this $Li-OH^-$ complex. An analogous defect has been observed at 3430 cm^{-1} in bulk MgO crystals and assigned to an OH^- ion adjacent to a lithium ion substituting for magnesium.[28,29]

In Fig. 5, we show possible models for the $Li-OH^-$ complex in the ZnO lattice. The primary experimental observations to be taken into account when constructing a model are (1) the alignment of the vibrating electric dipole along the *c* direction and (2) a peak position very near that of a free OH^- ion. When looking along the *c* axis in the wurtzite structure, one sees repeating anion-cation pairs. For example, each zinc ion has two adjacent *c*-axis oxygen ions as neighbors, one a close bonding oxygen and the other a more distant nonbonding oxygen. The lithium substitutes for a zinc in each of our models. In Fig. 5(a), we place the proton in an OH^- ion located at the lithium's nearest nonbonding oxygen site, with the proton facing the lithium. In Fig. 5(b), we place the proton in an OH^- ion located at the lithium's bonding oxygen site, with the proton extending out opposite the lithium. In the models illustrated in Figs. 5(a) and 5(b), only small amounts of lattice distortion are expected because, to first order, the proton occupies an interstitial position. Of these two models, the proton is closer to the lithium in Fig. 5(a) than in Fig. 5(b). In the absence of lattice distortion, these distances are about 2.26 and 2.95 Å, respectively, if an OH^- bond length of 0.96 Å is assumed. Thus, the model in Fig. 5(a) appears to be a better candidate than the model in Fig. 5(b) for the 3577.3-cm^{-1} band observed in the hydrothermally grown ZnO. In general, the interstitial proton would like to be close to the substitutional lithium because of their electrostatic attraction.

In Fig. 5(c), the proton is placed in the bond-center position between the lithium and its bonding oxygen. Although not depicted in the figure, this model will experience a severe lattice distortion, as illustrated in the earlier calculations of Van de Walle[1,7] (performed for the case when zinc is present instead of lithium). Based on those calculations, we expect that the lithium will move away from the proton and assume a position along the *c* axis near the plane of its remaining three oxygen neighbors. Without detailed calculations that explicitly include lithium, we cannot predict whether the defect configuration in Fig. 5(c) or Fig. 5(a) will have the lower energy. We note that the calculations in the literature thus far,[7] for zinc instead of lithium, favor the bond-center position in Fig. 5(c).

An estimate of the concentration of the OH^- ions contributing to the 3577.3-cm^{-1} band shown in Fig. 1 can be made. This requires a knowledge of the oscillator strength associated with the OH^- vibrational transition. Early predictions[46,47] of this oscillator strength ranged from 1.2×10^{-3} to 3.8×10^{-2}. Klauer *et al.*,[48] in a comprehensive and very detailed analysis of the OH^- ions in $LiNbO_3$ crystals, obtained a value of 1.7×10^{-2}. Taking a general approach, these latter investigators expressed their result as an absorption strength per ion. The concentration of OH^- ions *N* (in units of cm^{-3}) is then determined using the following equation:

$$\text{integrated area} = N\ (\text{absorption strength per ion}). \quad (1)$$

The absorption strength per ion has units of cm and the integrated area has units of cm^{-2}. If we use the value of $9.125\ (\pm1.369)\times10^{-18}$ cm provided by Klauer *et al.*[48] for the absorption strength per ion and a value of 6.9 cm^{-2} for the integrated area of the absorption band in Fig. 1, we ob-

tain a concentration N of 7.6×10^{17} cm^{-3}. Given that our values of the Hall electron carrier concentration and the photoinduced neutral lithium concentration (from EPR) are both in the low 10^{15}-cm^{-3} range, this result for N shows that over 99% of the lithium present in our sample has been compensated by hydrogen and has formed a Li–OH$^-$ defect.

V. SUMMARY

An infrared absorption band, caused by a defect with an electric-dipole moment aligned parallel to the c axis, has been observed near 3577.3 cm^{-1} in a hydrothermally grown crystal of ZnO. We assign this band to an OH$^-$ ion located on an oxygen site adjacent to a lithium ion substituting for a zinc ion. Two possible models are suggested. In one, the OH$^-$ is on a nonbonding oxygen site with the proton facing the lithium. In the other, the proton occupies a bond-center position, with significant lattice distortion causing the lithium to shift away from the OH$^-$ ion. *Ab initio* quantum calculations will be useful in deciding which model is correct. The concentration of the Li–OH$^-$ centers was estimated to be 7.6×10^{17} cm^{-3} in our sample. From these results, we conclude that one of the primary roles of hydrogen in ZnO is to provide charge compensation (and thus passivation) for singly ionized acceptors.

ACKNOWLEDGMENTS

This work was supported by the Air Force Office of Scientific Research (Grant No. F49620-02-1-0254 at West Virginia University and Lab Task 03SN07COR-5HC107 at Hanscom AFB) and monitored by Lt. Col. Todd Steiner. The authors would like to thank Chunchuan Xu for providing the Hall data.

[1]C. G. Van de Walle, Phys. Rev. Lett. **85**, 1012 (2000).
[2]C. G. Van de Walle, Physica B **308–310**, 899 (2001).
[3]C. G. Van de Walle, Phys. Status Solidi B **229**, 221 (2002).
[4]C. G. Van de Walle, Phys. Status Solidi B **235**, 89 (2003).
[5]D. M. Hofmann *et al.*, Phys. Rev. Lett. **88**, 045504 (2002).
[6]M. D. McCluskey, S. J. Jokela, K. K. Zhuravlev, P. J. Simpson, and K. G. Lynn, Appl. Phys. Lett. **81**, 3807 (2002).
[7]E. V. Lavrov, J. Weber, F. Borrnert, C. G. Van de Walle, and R. Helbig, Phys. Rev. B **66**, 165205 (2002).
[8]K. Ip *et al.*, Appl. Phys. Lett. **81**, 3996 (2002).
[9]B. Theys, V. Sallet, F. Jomard, A. Lusson, J. F. Rommeluere, and Z. Teukam, J. Appl. Phys. **91**, 3922 (2002).
[10]N. Ohashi, T. Ishigaki, N. Okada, T. Sekiguchi, I. Sakaguchi, and H. Haneda, Appl. Phys. Lett. **80**, 2869 (2002).
[11]E. V. Lavrov, Physica B **340–342**, 195 (2003).
[12]C. H. Seager and S. M. Myers, J. Appl. Phys. **94**, 2888 (2003).
[13]S. J. Jokela, M. D. McCluskey, and K. G. Lynn, Physica B **340–342**, 221 (2003).
[14]N. H. Nickel and K. Fleischer, Phys. Rev. Lett. **90**, 197402 (2003).
[15]N. Ohashi, T. Ishigaki, N. Okada, H. Taguchi, I. Sakaguchi, S. Hishita, T. Sekiguchi, and H. Haneda, J. Appl. Phys. **93**, 6386 (2003).
[16]A. Y. Polyakov *et al.*, J. Appl. Phys. **94**, 2895 (2003).
[17]K. Ip *et al.*, Appl. Phys. Lett. **82**, 385 (2003).
[18]A. Y. Polyakov *et al.*, J. Appl. Phys. **94**, 400 (2003).
[19]Y. M. Strzhemechny, J. Nemergut, P. E. Smith, B. Junjik, D. C. Look, and L. J. Brillson, J. Appl. Phys. **94**, 4256 (2003).
[20]N. H. Nickel and K. Brendel, Phys. Rev. B **68**, 193303 (2003).
[21]Y. M. Strzhemechny *et al.*, Appl. Phys. Lett. **84**, 2545 (2004).
[22]M. Sano, K. Miyamoto, H. Kato, and T. Yao, J. Appl. Phys. **95**, 5527 (2004).
[23]E. Mollwo, G. Muller, and D. Zwingel, Solid State Commun. **15**, 1475 (1974).
[24]D. Zwingel, Phys. Status Solidi B **67**, 507 (1975).
[25]G. Muller, Phys. Status Solidi B **76**, 525 (1976).
[26]D. Zwingel, Solid State Commun. **26**, 779 (1978).
[27]E. Ohshima, H. Ogino, I. Niikura, K. Maeda, M. Sato, M. Ito, and T. Fukuda, J. Cryst. Growth **260**, 166 (2004).
[28]R. Gonzalez, R. Pareja, and Y. Chen, Phys. Rev. B **45**, 12730 (1992).
[29]R. Gonzalez, I. Vergara, D. Caceres, and Y. Chen, Phys. Rev. B **65**, 224108 (2002).
[30]M. J. Callahan, D. F. Bliss, M. T. Harris, and M. N. Alexander, in *Properties, Processes and Applications of ZnO*, edited by C. W. Litton, D. C. Reynolds, and T. C. Collins (IEE IOP, London, 2004), Chap. 8.
[31]P. Koidl, Phys. Rev. B **15**, 2493 (1977).
[32]H. J. Schulz and M. Thiede, Phys. Rev. B **35**, 18 (1987).
[33]W. M. Walsh and L. W. Rupp, Phys. Rev. **126**, 952 (1962).
[34]A. Hausmann and H. Huppertz, J. Phys. Chem. Solids **29**, 1369 (1968).
[35]A. Hausmann, Phys. Status Solidi **31**, K131 (1969).
[36]W. C. Holton, J. Schneider, and T. L. Estle, Phys. Rev. **133**, A1638 (1964).
[37]J. Schneider and A. Rauber, Z. Naturforsch. A **16**, 712 (1961).
[38]N. Y. Garces, L. Wang, L. Bai, N. C. Giles, L. E. Halliburton, and G. Cantwell, Appl. Phys. Lett. **81**, 622 (2002).
[39]O. F. Schirmer, J. Phys. Chem. Solids **29**, 1407 (1968).
[40]O. F. Schirmer and D. Zwingel, Solid State Commun. **8**, 1559 (1970).
[41]D. Zwingel, J. Lumin. **5**, 385 (1972).
[42]N. Y. Garces, L. Wang, M. M. Chirila, L. E. Halliburton, and N. C. Giles, Mater. Res. Soc. Symp. Proc. **744**, 87 (2003).
[43]J. C. Owrutsky, N. H. Rosenbaum, L. M. Tack, and R. J. Saykally, J. Chem. Phys. **83**, 5338 (1985).
[44]M. Wohlecke and L. Kovacs, Crit. Rev. Solid State Mater. Sci. **25**, 1 (2001).
[45]S. J. Pearton, J. W. Corbett, and M. Stavola, *Hydrogen in Crystalline Semiconductors* (Springer, Berlin, 1992).
[46]O. W. Johnson, J. DeFord, and J. W. Shaner, J. Appl. Phys. **44**, 3008 (1973).
[47]R. Richter, T. Bremer, P. Hertel, and E. Kratzig, Phys. Status Solidi A **114**, 765 (1989).
[48]S. Klauer, M. Wohlecke, and S. Kapphan, Phys. Rev. B **45**, 2786 (1992).